

International Conference on Space Optics—ICSO 2022

Dubrovnik, Croatia

3–7 October 2022

Edited by Kyriaki Minoglou, Nikos Karafolas, and Bruno Cugny,



Piezoelectric and Magnetic Fast Steering Mirrors for Space Optical Communication



Piezoelectric and Magnetic Fast Steering Mirrors for Space Optical Communication

G. Aigouy ⁽¹⁾, A. Guignabert ⁽¹⁾, E. Betsch ⁽¹⁾, H. Grardel ⁽¹⁾, P. Personnat ⁽¹⁾, J.M Nwesaty ⁽¹⁾, X. De-Lepine ⁽¹⁾, A. Bedek ⁽¹⁾, A. Baillus ⁽¹⁾, N. Bourgeot ⁽¹⁾, F. Claeysen ⁽¹⁾

(1) CEDRAT TECHNOLOGIES, 59 Chemin du Vieux Chêne, Inovallée, 38246 MEYLAN
Cedex France, gerald.aigouy@cedrat-tec.com

ABSTRACT

New space giant constellations based on Free-Space Optical Communication (FSO) are a new challenge from many perspectives. Considering the mandatory cost efficiency, with repeatability of performances, and reliability with no defect at customer integration, requires an upheaval in space production and acceptance test methods, when the quantities are beyond several thousands of units.

In this publication CEDRAT TECHNOLOGIES (CTEC) presents the design and test results of the P-FSM150S Pointing Ahead Mechanism (PAM) and M-FSM45 Fast Steering Mirror (FSM) Engineering Models, developed under ARTES project TELCO-B for future FSO constellations. The specific cost-efficient hardware design is presented, dedicated to very large quantities to be manufactured, together with the performance test results over a preliminary batch of EM's production.

Keywords: Optical Communication, Free-Space Optics, Fast Steering Mirrors, Pointing Ahead Mechanisms, Fine Pointing Mechanisms, Strain Gauges Position Sensors, Eddy Current Position Sensors.

1. P-FSM150S & M-FSM45 SIC MIRRORS

Two mirrors have been designed and tested for both the P-FSM150S and M-FSM45. Both mirrors have been designed in silicon carbide (SiC) material, according to CTEC heritage on NASA/PSYCHE PAM30 project [1,2], and have been successfully tested before and after integration on each mechanism.

1.1 Silicon Carbide (SiC) Mirrors design

One of the main design constraints of an opto-mechanism is to avoid any mirror surface deformation at integration onto the mechanical parts, in order to warranty an optical wave front error lower than the application requirements. As a cost compromise objective, the reflected wave front error (RWE) after integration was targeted lower than 40nm rms at 0° angle of incidence, corresponding to a mirror surface optical flatness lower than 20nm rms.

The opto-mechanical design has been optimized by CTEC, based of former space flight heritage methodology, for the finite element analysis of the mirror surface deformation caused by mechanical biases at integration, and by thermo-mechanical deformation over the application temperature range [-10°C, +60°C].

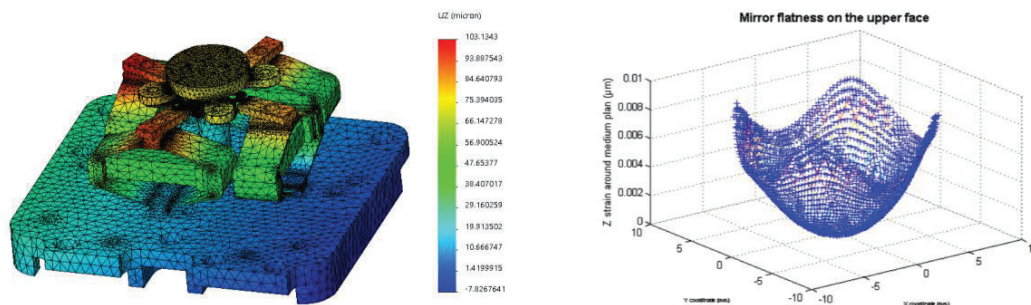


Figure 1. P-FSM150S simulation (vertical displacement & mirror deformation) for a +60°C temperature

For both mechanisms, specific mirrors, and flexible mirror supports, were designed and optimized. The mirror flexible support being a key component, avoiding any mirror deformation at integration, and during temperature variations, while keeping an actuation mechanism stiff enough to withstand vibrations and shocks launch loads, as well as actuators parasitic forces. The mirror deformation induced by the mechanism actuation cumulated to temperature variations, was targeted lower than 20nm rms RWE, together with a mirror RWE targeted also lower than 20nm rms at manufacturing, with appropriate optical coating, leading to a total RWE lower than 40nm rms at any operational condition. This objective was successfully achieved with margin.

1.2 Mirrors procurement and verification

The 2 mirror designs were manufactured for the engineering models (3 EM's of each), and the optical acceptance test were performed by CTEC before and after integration. The following pictures shows the mirrors RWE (reflected wave front error) measured with a Zygo interferometer at CTEC laboratory.



Figure 2. Mirror type 1 & silver coating (left), type 2 & gold coating (middle), and RWE tests after integration (right)

After both mechanism assembly (P-FSM150S and M-FSM45), the mirror surface flatness was controlled. The optical verification indicates that both mirrors were compliant with important margins in both free state and after integration. The RWE of M-FSM45 mirror is a bit better than the P-FSM150S because its mirror is thicker.

	P-FSM150S	M-FSM45
Mirror RWE before integration (nm rms)	14.2	10
Mirror RWE after integration (nm rms)	17.5	12.7

Table 1. Mirror optical control results (specification: RWE < 40nm rms @ 633nm)

2. P-FSM150S POINT AHEAD MECHANISM (PAM) DESIGN AND MANUFACTURING

The main specifications for this mechanism were to ensure an angular stroke of +/-7 mrad throughout the full operational temperature range of the mission (-10/+60°C) and a mirror surface flatness under 40nm rms RWE (Reflected Wavefront Error) while remaining inside a very limited volume (especially less than 30mm height) and surviving launch vibrations.

2.1 P-FSM150S Mechanism design overview

The piezo actuators are cabled in 2 push-pull configurations (1 driving channel per axis) to allow a direct mirror rotation control, inheriting from PHARAO and ATLID tip-tilt mechanisms [3,4].

The P-FSM150S itself is composed of the following parts:

- A bracket baseplate (in aluminum)
- 4 APA® actuators (in stainless steel)
- 4 Strain gauges (SG) position sensors located onto the APA® actuators
- A mirror flexible support (in stainless steel), providing all in one both flexible mirror mounting and tilting flexure bearing, insuring perfect mirror rotation control without deformation.
- A central cylinder support soldered with the flexure bearing that stiffens the assembly.
- A Silicon Carbide substrate-based mirror (SiC or SiSiC)



Figure 3. PFSM-150S Engineering Model (left) & Strain Gauge onto piezo ceramic (right)

2.2 P-FSM150S Strain Gauge position sensors (SG)

In order to be able to monitor the mirror angle, an indirect solution using strain gages placed on each piezo actuator is selected, based space heritage from other projects, especially ATLID [4] on this matter, which enabled an important development on SG assembly process.

The project used constantan, 350Ohm SG. There is 1 SG per piezo stack, mounted in one full Wheatstone bridge per rotation axis to maximize the sensitivity while minimizing thermal drift. All SG wires and PCB traces are the same length to limit offset drift.

2.3 P-FSM150S New APA® piezo actuator design

The mechanism is composed of 4 APA®, deriving from CTEC standard APA120S. The existing CTEC actuators were either slightly too short in stroke or not stiff enough to ensure the mechanism survival during the launch. Therefore, APA150S have been specifically designed for the application needs.

A total of 25 APA® were assembled and tested, the measurements are detailed in the following table:

	Full stroke (-20/+150V)	1st resonant frequency (actuation)
Units	µm	Hz
Average (measured)	187.3	4892.0
Standard deviation (measured)	0.9	22.9
Design value (worst case)	152.8	4783
Difference measurement/design value	+23%	+2%

Table 2: P-FSM custom APA measurement results

2.4 P-FSM150S Manufacturing and assembly

Four P-FSM150S EM have been assembled (EM1 to EM4). The integration process and assembly tooling was constantly improved as the operations were progressing. Even for prototypes, one of the focus was to keep the time required to assemble the model as low as possible, in anticipation with the aim to have this mechanism compatible with serial production.

Hence the number of steps, especially highly time-consuming ones like gluing, was reduced to the minimum required without impacting required quality.

With that in mind, each integration step duration was monitored, and the overall process time was analyzed in order to identify critical steps and room for process optimization.

3. P-FSM150S TEST RESULTS

3.1 P-FSM150S Stroke and Modal Actuation Frequencies Test Results

As it was anticipated based on the good piezo actuators stroke performance (see Table 2), the P-FSM150S mirror tilt angle range is compliant with the requirements, with notable operational margins. Hence the target stroke of ± 7 mrad can even be reached (at ambient temperature) supplied with a limited voltage range of $0/+130$ V instead of $-20/+150$ V (23% less voltage).

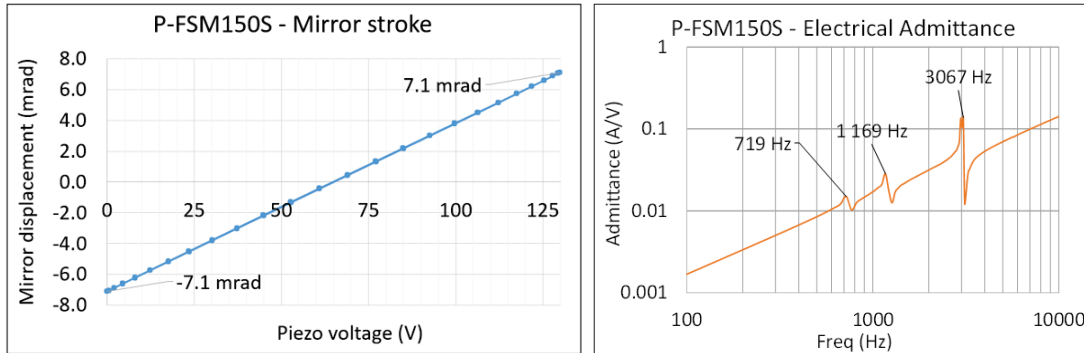


Figure 4. PFSM150S stroke results with a $0/+130$ V (left) supply & admittance sweep (right)

The actual full operational stroke could not be fully tested due to the limited range of the autocollimator instrument, but we can extrapolate that the PFSM could reach a ± 9.6 mrad stroke with a $-20/+150$ V supply, which should cover the slight stroke loss expected in cold operational temperature (around -5%) and the mirror integration offset compensation.

The mechanism stiffness and associated modal landscape is evaluated with an admittance sweep. With that method, only the piezo coupled modes are visible, hence the vertical pumping mode (cancelled from piezo point of view) is not visible. The first mode measured at 719 Hz corresponds to the X axis mirror tilt, the main actuation mode. The modal simulations results evaluated the tilt modes at 738 Hz, the result is then quite close to the simulation (-2.6%), the difference coming from model approximations, material uncertainties and parts machining tolerances.

3.2 P-FSM150S Cross Coupling and Resolution Tests Results

The tests reveal a 0.1% cross coupling (prior cancellation by closed loop position control): ± 10 μ rad cross axis displacement with a ± 7 mrad stroke which is a good result given the high amplification of the mechanism. With another test, it is demonstrated that the mechanism can generate ± 1 μ rad steps (0.01% mechanical resolution), using an external measurement for the mirror angle (autocollimator). The share of errors due to instruments measurement has still to be determined (especially for cross coupling) but measured resolution is already compliant with the ± 1 μ rad specification.

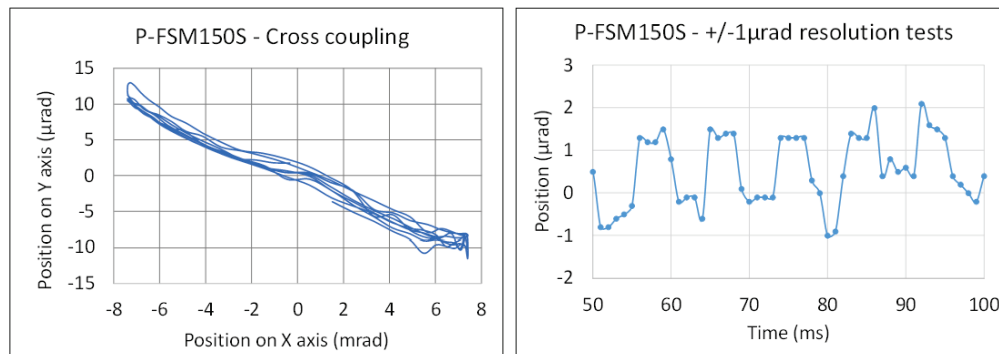


Figure 5. PFSM150S cross coupling (Left) and resolution (right) measurement tests

3.3 P-FSM150S SG Position Sensor Accuracy test results

The SG position sensor being an indirect measurement method based on the calibration of the piezo-ceramic deformation versus the angular motion, the piezo-ceramic hysteresis impacts the position measurement accuracy with a linearity error. The linearity error was measured at +/- 0,5% of stroke, which correspond at +/- 7mrad full stroke to an error of +/- 35µrad. The SG position sensor being the most compact and best cost-efficient approach for large scale quantities, no alternate embedded sensor was proposed during this project. Anyway, alternate direct position measurements method can be implemented onto this mechanism, such as eddy current sensors (ECS) as per M-FSM45, or optical sensors, but with higher cost and dimension penalties.

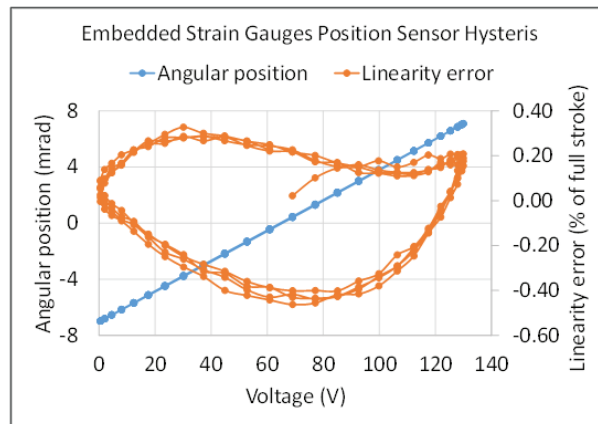


Figure 6. PFSM150S SG position sensors linearity measurement

3.4 P-FSM150S Closed Loop Position Control Test Results

The P-FSM150S closed loop position control test was achieved with a low power drive electronics, for pointing ahead mirror (PAM) application, with a low speed basic proportional Integral (PI) controller. The tuning of the controller was designed to be compatible with very low power drive electronics, which is a major objective and constrain for large scale space constellation to reach high cost efficiency.

A frequency bandwidth of 727Hz was achieved with a 1 ms step and stay position settling time.

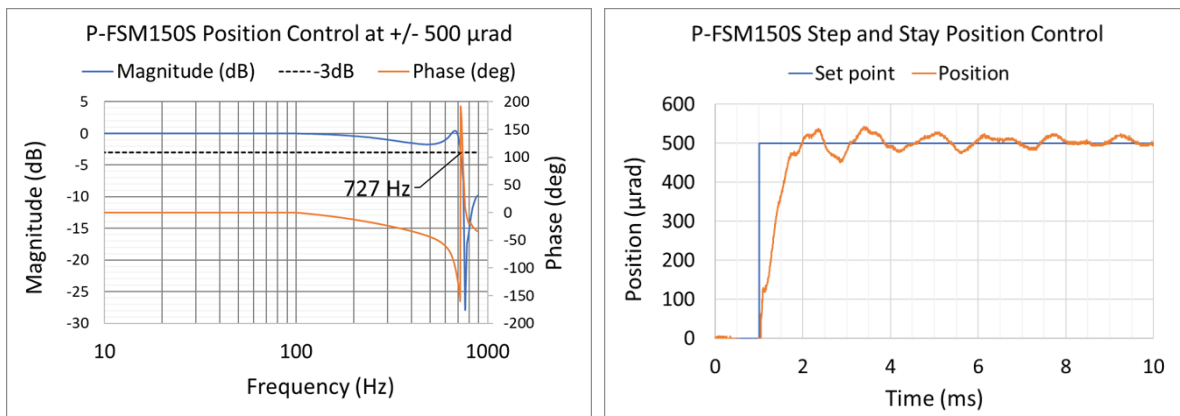


Figure 7. PFSM150S Closed loop feed-back position control

3.5 P-FSM150S Accelerated Fatigue Lifetime Tests

The EM1 is currently going through a lifetime test. The mechanism was first started in June 2021 at full stroke ($\pm 7\text{mrad}$) in diagonal direction (45° along x and Y axis) to excite both axis in fatigue, and with a frequency of 100Hz. With this test condition, the first billion cycles have been reached after the 4 firsts months. After that period, the test frequency was accelerated to 400Hz, which has allowed to achieve at publication time frame more than 5.10^9 cycles, still on going. The lifetime test shall be continued up to failure, and will be regularly interrupted to evaluate any loss of performance over lifetime. 15 years fatigue lifetime is expected to be demonstrated in less than two years accelerated test, with one year already achieved by June 2022, i.e. already half the way successfully achieved without any loss of performance.

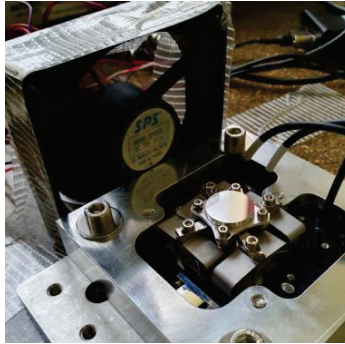


Figure 8: Lifetime test set-up for PFSM150S EM1

3.6 P-FSM150S Random Vibrations and SRS Shock Tests Results

The P-FSM150S was tested in random vibrations, and SRS shocks, respectively at $0,65\text{g}^2/\text{Hz}$ (at its first structural resonance frequency at 720Hz), and 1500g at drop test shock impact, with ISO8 clean condition packaging.

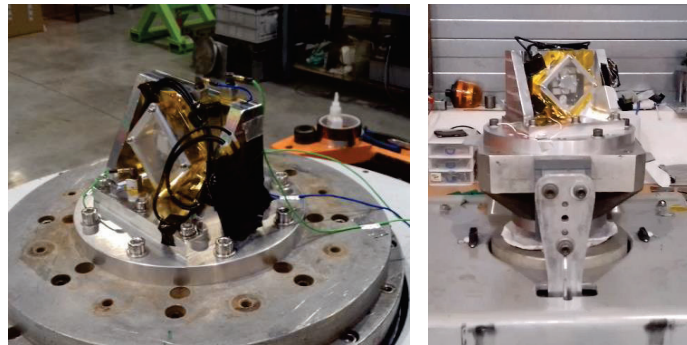


Figure 9: Random vibrations (left), and Shock (right), test set up in clean ISO8 condition packaging

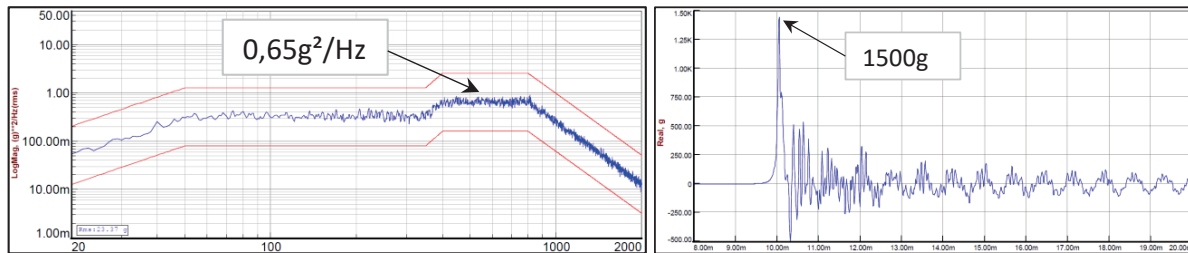


Figure 10: P-FSM150S $0,65\text{g}^2/\text{Hz}$ Random Vibrations test (left) and 1500g Shock test impact transient (right)

The P-FSM150S was shock tested with a drop machine in order to test a 800g SRS shock input level at 1000Hz. In order to achieve the targeted test input all along the specified SRS frequency spectrum, the level was exceeded up to 1500g at drop impact, which resulted in a tested SRS spectrum here under (blue), much higher than the specification (green).

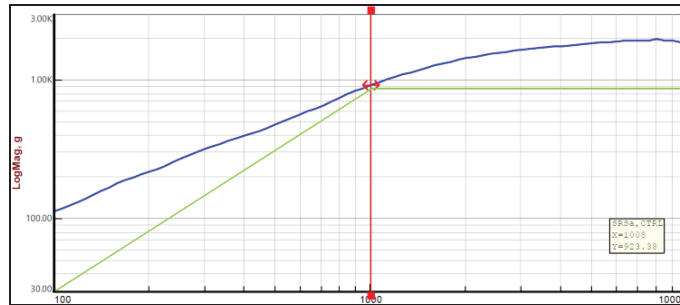


Figure 11: P-FSM150S 1500g SRS Shock Test – SRS analysis

3.7 P-FSM150S expected reliability figures

CTEC has a long heritage in Optronics domain, with the delivery of 3430 XY piezo stages based on similar push-pull piezo-mechanism, and with fluctuating production rate from 200 to 500 per year (i.e. 20 to 50 month).

Since 2005 this production has been delivered to several customers, with custom design for each on interfaces, connectors, and optical components.

The production rate, and test acceptance approach, are based on this heritage, to guarantee a zero defect at customer level and 100% testing before delivery.

Over this historical of quantity delivered, only one failure was observed, and has led to a customer service, which had concluded on a customer mistake at integration and not as a hardware defect. The Piezo stage was sent back to customer without modification.

Considering anyway this single event as a failure to be conservative, the following reliability analysis can be performed:

- ✚ Cumulated operational hours = 1,33.107 at 20°C and average voltage @ 65V
- ✚ Failures in Time (FIT) = 75 over 1 billion hours
- ✚ Reliability **R= 0,992**

4. M-FSM45 FAST STEERING MIRROR (FSM) DESIGN AND MANUFACTURING

4.1 M-FSM45 Mechanism and Magnetic design overview

The M-FSM45 is a magnetic mechanism driving two tilt axes on a large angle requirement. This FSM, which derives from M-FSM62 [5,6] is composed of the following parts:

- A Magnetic circuit in Soft Magnetic Composite material with 4 magnets and a moving part.
- 4 Coils optimized to provide the best induction in the short volume, with potting to dissipate the generated heat.
- An Eddy Current Sensor device with aluminium targets embedded on the moving parts, and 4 sensing heads on a single PCB below.
- A moving part suspended on a flexure bearing ensuring high lifetime performances.
- A mirror fixed on a flexible baseplate limiting the integration deformations.

The magnetic design relies on forces due to tangential variable magnetic reluctance, which offers higher forces than Lorentz forces [7] and more linear forces than normal variable magnetic reluctance [8].

To ensure the FSM performances, magnetic calculations by FEA have been performed. The magnetic saturation, available torque and parasitic forces were verified.

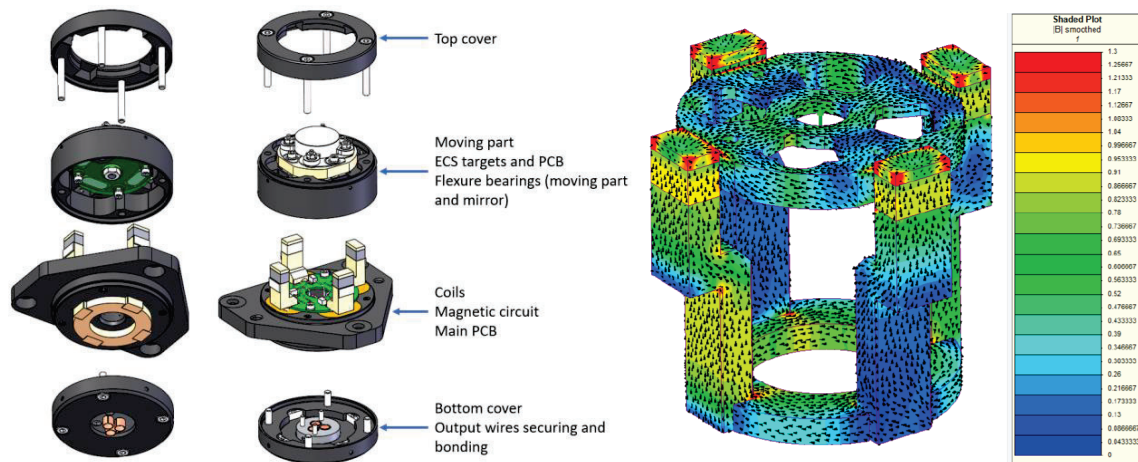


Figure 12: M-FSM cost efficient design concept (left) and magnetic circuit finite element modelling (right)

4.2 M-FSM45 Eddy Current Position Sensors (ECS)

To measure the mirror position and perform closed loop control, an eddy current sensor assembly is embedded in the mechanism. The sensor assembly is eased thanks to the design of a single PCB including the 4 sensing coils, taking advantage of space qualification of PCB-ECS sensors [9]. This solution makes the M-FSM more compact, with an efficient one step assembly. The sensitivity has been optimized for the FSM stroke, making the sensor non-linearity acceptable for the application.

4.3 M-FSM45 Manufacturing and Assembly

The mechanism design has been optimized with the objective of reducing the assembly complexity and time, in order to achieve high cost efficiency for very large quantities production. Specific tooling was designed for critical steps such as mirror integration, coils' potting, or moving part assembly into the magnetic circuit.

The magnetic parts were manufactured by industrial molding processes, dedicated to composite magnetic material featuring very low eddy currents. The geometrical tolerances were considered by design to sustain the worst-case air gaps in the torque calculation.

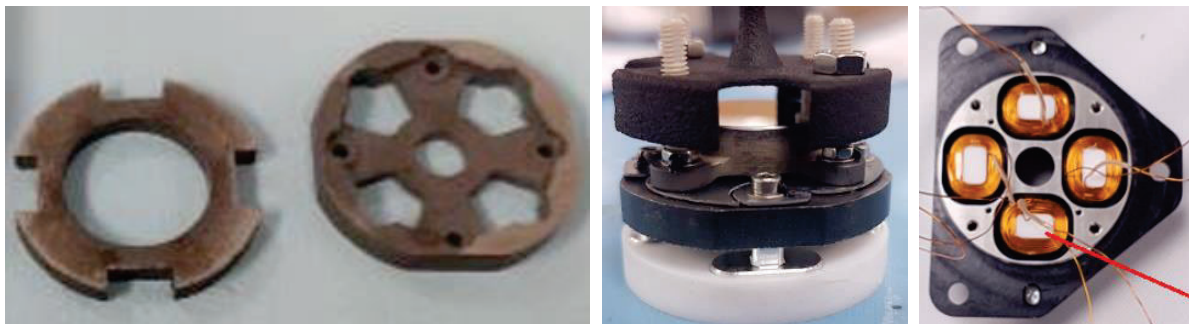


Figure 13: M-FSM SMC parts (left), tooling for mirror & moving part (center), and coils' assembly (right)



Figure 14: M-FSM45 Engineering Model N°1

5. M-FSM45 TEST RESULTS

5.1 M-FSM45 Stroke and ECS Position Sensors' accuracy Test Results

The stroke measured shows that the M-FSM is allowing a maximal stroke slightly lower than $\pm 1.5^\circ$ ($\pm 25.8\text{mrad}$) for a $\pm 1\text{A}$ current input. The measurements have been performed thanks to a large angle autocollimator allowing a single angle low frequency acquisition.

After complete assembly of the M-FSM45 the ECS position sensors accuracy was measured compared to the optical measure of mirror position with an autocollimator facility. The accuracy error of ECS position sensors was in the range of $\pm 0,08\%$ of the $\pm 15\text{mrad}$ measurement full scale.

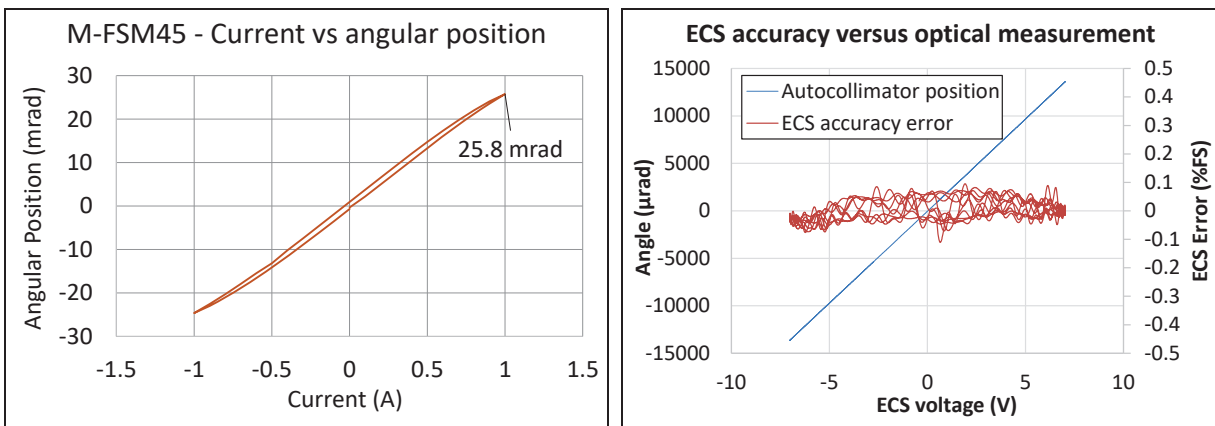


Figure 15: M-FSM45 stroke amplitude test (left) and ECS sensors test (right)

5.2 M-FSM45 Electrical Performance Tests Results

The M-FSM45 was designed to be compatible with a space drive electronics with maximum voltage of 24V voltage and 0,5A current for a +/-500 μ rad set point at high frequency.

The following measurement results shows the electrical margins with maximum voltage of 16V and maximum current at 0,7A, achieved at 500Hz.

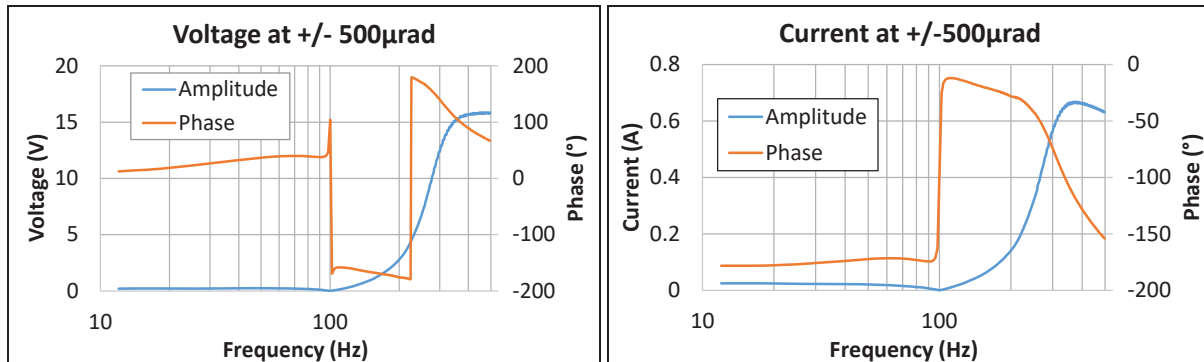


Figure 16: M-FSM45 voltage measure (left) and current measure (right) @ +/-500 μ rad

The following plots shows the electrical impedance measurements achieved onto the mechanism after full assembly. The following plots show the apparent resistance and inductance which vary with increase of frequency due to Eddy current losses.

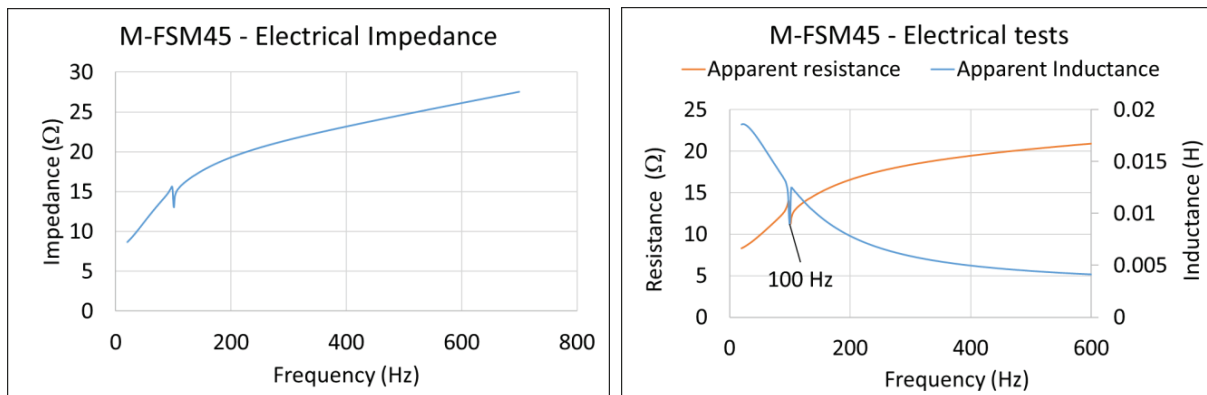


Figure 17: M-FSM45 electrical impedance tests

The Eddy currents losses were analyzed by subtraction from total active power absorbed by the M-FSM45 with the Joules losses. The following plots shows the electrical power measurement and losses analysis versus frequency at +/- 500 μ rad angle amplitude. The electrical power is very low up to 200Hz with less than 0,2W and then increases starting from 200Hz up to 4W at higher frequencies and up to 500Hz.

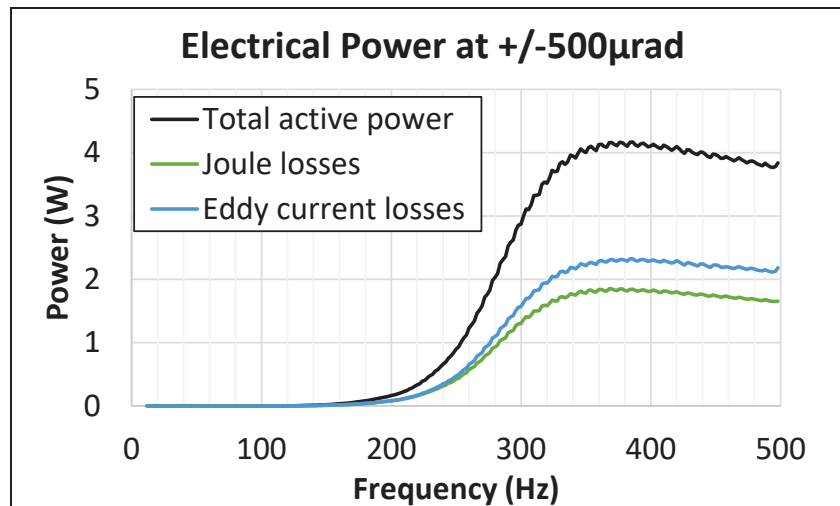


Figure 18: M-FSM45 Electrical power test @ +/-500µrad

5.3 M-FSM45 Closed Loop Position Control Development on M-FSM62

The development of the position feed-back closed loop control on the M-FSM technology, has been achieved onto the M-FSM62 which is a much bigger FSM, and was then implemented and tuned onto the M-FSM45. The presented position feed-back control of M-FSM's is based on the embedded ECS position sensors.

The test with closed loop control allows to measure the mechanical performances, as well as all the electrical driving performances, with drive electronics having representative limits w.r.t flight ones, in terms of voltage, current, power, and closed loop controller tuning.

The following picture shows the closed loop position feed-back control test bench, using both internal ECS position sensors and external optical instrumentation (autocollimator and PSD) using a laser pointing source.



Figure 19: M-FSM62 on optical & closed loop control test bench

The M-FSM62 frequency bandwidth could be measured at several stroke amplitudes, up to +/-25mrad, and one can see that -3dB bandwidth was measured at 146Hz.

The drive electronic used for the test was the MCSA480 which provides a maximum current rated at 10A, with safety hardware shut down beyond. The following picture shows the stroke amplitude that was achievable versus frequency up to the reaching of maximum limit of electronic shut down (hardware shut down curve).

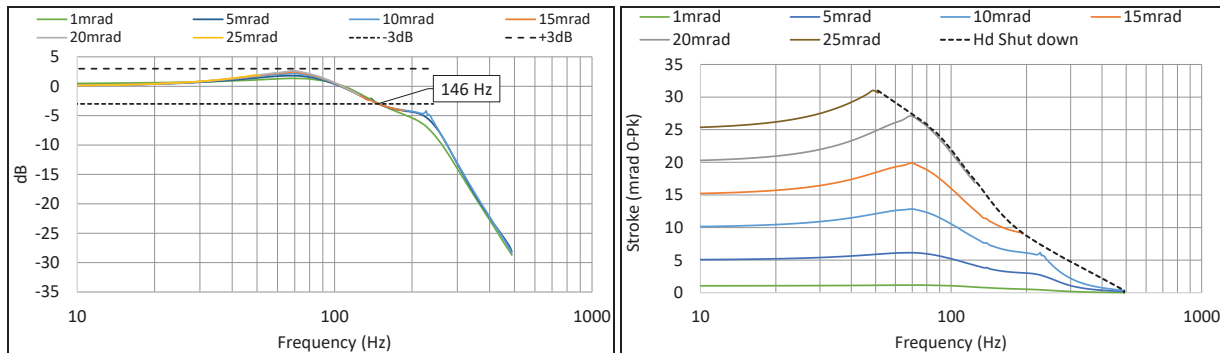


Figure 20: M-FSM62 Bandwidth tests at different amplitudes (left) and Amplitude diagrams v.s electronics limits (right)

The advantage of the MCSA480 is its high electrical power rating, which allows testing a magnetic FSM far beyond its resonance frequency and at high power. This result is of high interest, because the required power in order to achieve high stroke at frequencies higher than the resonance frequency dramatically increases. One can see in the following plot that ± 25 mrad at 50Hz driving frequency requires only 2,5W on the M-FSM62, whereas driving frequencies higher than 200Hz requires about 50W for maximum reachable stroke amplitude about ± 6 mrad.

The measured electrical active power absorbed by the M-FSM62, was analyzed w.r.t coil Joule effect, and in Eddy currents losses, which result both in heating onto the M-FSM. This analysis here under shows the results for a stroke amplitude of ± 10 mrad, which is considered as relevant target for flight. One can see that under 100Hz the total electrical active power absorbed is lower than 0,5W with Eddy currents losses increasing versus frequency, and becoming comparable to coil Joule losses for frequencies beyond 100Hz, leading to 50W total power consumption at 200Hz with ± 6 mrad of stroke achievable. This illustrates the power effort required for the driving of a magnetic FSM far beyond its resonance frequency, which is not a trivial result.

The M-FSM45 mirror and moving mass being much smaller compared to M-FSM62, and together with a better optimization w.r.t Eddy current losses (shape and materials) the M-FSM45 power consumption at high frequency is much smaller.

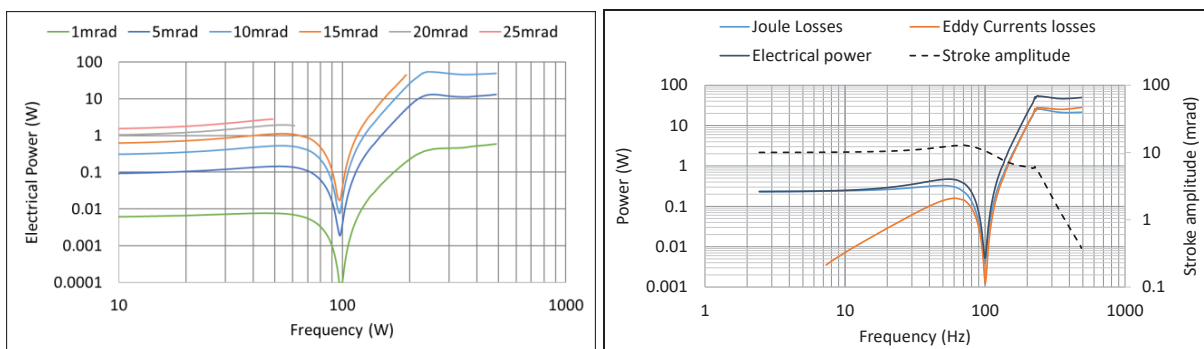


Figure 21: M-FSM62 Power diagrams (left) and Eddy current losses +/-10mrad amplitude (right)

5.4 M-FSM45 Closed Loop Position Control Test Results

After development onto the M-FSM62 the position control method was implemented onto the M-FSM45, with lower moving mass, which has resulted in higher frequency bandwidth. The frequency bandwidth test was achieved at +/- 500µrad position amplitude and has shown an increase of -3dB frequency bandwidth from 146Hz on M-FSM62 to 320Hz on M-FSM45, which is considered a very good result.

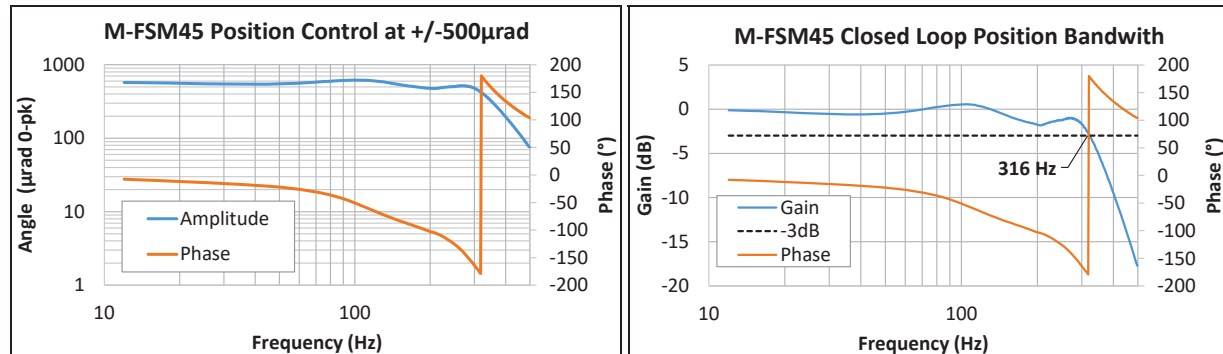


Figure 22: M-FSM45 closed loop position control test

5.5 M-FSM45 and M-FSM62 tests results comparison

The results from both M-FSM62 and M-FSM45 have allowed to evaluate size impact of M-FSM technology, which is an important result if one considers sizing extrapolation, and dimension optimization. The M-FSM45 achieves a much lower power consumption and higher bandwidth compared to M-FSM62 due to smaller moving mass, and angle stroke rating. As a relevant summary the following table present the difference of performance of both M-FSM sizes.

	M-FSM62	M-FSM45
Mirror aperture	30mm	15mm
Housing Diameter	62mm	46mm
Height	56mm	35mm
Mass	400g	195g
Stroke amplitude	+/- 50mrad (1)	+/- 25mrad
Resonance freq.	100Hz	100Hz
Rated voltage	40V	12V
Rated current	10A	0,5A
Rated power for freq. < 100Hz	2,5W	0,2 W
Max. rated power for freq. > 100Hz	50W	5 W
-3dB Bandwidth @ Full stroke	145 Hz	320 Hz

(1) Reduced to +/- 25mrad with embedded ECS position sensor option.

Table 3: M-FSM62 & M-FSM45 test results summary

6. P-FSM150S AND M-FSM45 DESIGN AND TEST RESULTS SUMMARY

The following table summarizes the design data and test results of both P-FSM150S and M-FSM45, both design in order to achieve high cost efficiency, and high reliability.

	P-FSM150S	M-FSM45
Dimensions	65mm x 60mm; H 30mm	Φ 46mm; H 35mm
Mass	150 g	195 g
Stroke at [0V, +130V] voltage range	+/- 7 mrad	--
Stroke at [-20V, +150V] voltage range	+/- 9 mrad	--
Stroke at [-12V, +12V] voltage range	--	+/- 25 mrad
Rated current	< 0,01A	1 A
Maximum static power (full stroke step & stay)	< 0,001 W	8W
Power @ +/- 500μrad for frequencies < 100Hz	< 0,05 W	< 0,2 W
Power @ +/- 500μrad for frequencies > 100Hz	< 0,5 W	< 5 W
Actuation resolution (1)	+/- 1 μrad	+/- 1 μrad
Sensor accuracy (1)	< +/- 40μrad	< +/- 2μrad
Embedded position sensors	Strain gauges (SG)	Eddy Current Sensors (ECS)
1st resonance frequency (Actuation)	720 Hz	100 Hz
Closed loop position control Frequency bandwidth	> 700 Hz (2)	> 300 Hz (3)
Mirror size	Ø15mm clear aperture	Ø15mm clear aperture
Mirror substrate (4)	SiC or SiSiC	SiC or SiSiC
Mirror coating	Silver coating or Gold coating	Silver coating or Gold coating
Mirror mechanical interface onto support	Fastening (5)	Fastening (5)
Mirror RWE after integration on flexible support	< 20nm rms (6)	< 20nm rms (6)
Operational temperature	-10°C / +60°C	-10°C / +60°C
Random vibration level	0,65g ² /hz from 100Hz to 800Hz	Not tested yet
SRS shock level	1000g from 1000Hz to 10000Hz	Not tested yet

(1) With non-space cots drive electronics

(2) For low speed fine pointing operation and very low electrical power drive electronics. Much higher frequency bandwidth is achievable with higher power drive electronics for fast steering operation.

(3) For fast steering operation at large full stroke

(4) The mirror flexible support is compatible with other alternate metallic substrates, w.r.t WFE after integration, , with same usable mirror mechanical drawing applicable

(5) Mirror gluing processes avoided for fast and reliable assembly processes

(6) At 0° angle of incidence and 633 nm

7. ACKNOWLEDGEMENT AND CONCLUSION

This development was achieved during the TELCO-B ARTES project under the funding of CNES and ESA. The authors particularly thanks Thales Switzerland, CNES and ESA, which have allowed the bringing to maturity of P-FSM150S and M-FSM45 as candidate flight products for future large-scale space constellations.

REFERENCES

- [1] A. Guignabert, Point Ahead Mechanism for Deep Space Optical Communication for PSYCHE mission, Proc. ICSO, February 2021
- [2] A. Guignabert, Point Ahead Mechanism for Deep Space Optical Communication – Development of a new Piezo-Optical Tip-tilt mechanism, Proc AMS, Houston, May 2020
- [3] R. Le Letty, Miniature Piezo Mechanisms for Optical and Space applications, ACTUATOR Conf, Messe Bremen (G), June 2004, pp 177-180
- [4] F. Claeysen, Beam Steering Mirrors from space applications to optronic solutions, Proc. OPTRO Conf, Paris, Feb. 2018
- [5] F. Claeysen, Large-stroke Fast Steering Mirror for space Free-Space Optical communication, OPTRO 2020, n°0062, 28-30 Jan 2020
- [6] A. Guignabert, E. Betsch, G. Aigouy, Large stroke Fast Steering Mirror, Proc. ICSO, February 2021
- [7] W. Coppoolse, Dual-axis single-mirror mechanism for beam steering and stabilisation in optical inter satellite links, Proc ESMATS conf, 2003
- [8] Y. Long, Design of a Moving-magnet Electro magnetic Actuator for Fast Steering Mirror, J. of Magnetism, Vol. 19 (3), 2014
- [9] JC Barriere, Qualification of euclid-near infrared spectro-photometer cryomechanism, Proc. ESMATS 2017